Acta Cryst. (1980). B36, 774–782

FeB–CrB Stacking Variations for Rare-Earth–Nickel Alloys in Quasi-Binary Sections $R_{1-x}R'_xNi$

BY K. KLEPP AND E. PARTHÉ

Laboratoire de Cristallographie aux Rayons X, Université de Genève, 24 quai Ernest Ansermet, CH-1211 Genève 4, Switzerland

(*Received* 30 *October* 1979; *accepted* 3 *December* 1979)

Abstract

In the quasi-binary systems GdNi–YNi and GdNi–DyNi mixed stacking variants of the FeB and the CrB types have been found. They all have monoclinic symmetry with space group $P2_1/m$. $Gd_{0.75}Y_{0.25}Ni$ with base-structure stacking h_2c_3: a = 18·20 (1), b = 4·212 (2), c = 5·506 (1) Å, β = 102·37 (5)°, Z = 10, R = 0·043. $Gd_{0.55}Dy_{0.45}Ni$ with base-structure stacking h_2c_2: a = 14·35 (2), b = 4·217 (1), c = 5·468 (1) Å, β = 100·39 (4)°, Z = 8, R = 0·033. $Gd_{0.7}Y_{0.3}Ni$ with base-structure stacking h_2c: a = 10·76 (1), b = 4·194 (1), c = 5·508 (1) Å, β = 96·98 (4)°, Z = 6, R = 0·089. The geometrical conditions required for stacking variants are discussed; these lead to simple unit-cell relationships. The quasi-binary phases between the FeB and CrB end members may be characterized by the ratio of FeB- to CrB-type fragments in the structures. This ratio depends on the composition. Structures of compounds closer to the binary compound with FeB type have more FeB- than CrB-type fragments in their structure and *vice versa*.

Introduction

The equiatomic compounds formed between rare-earth elements and transition elements of Group VIII or *B* elements (those with filled *d* shells) of Groups I to IV crystallize with the FeB, CrB or CsCl structure types. The FeB and CrB structure types are characterized by trigonal prisms of rare-earth atoms centred by the alloying partner while the CsCl type can be described as an arrangement of centred cubes. A survey of the crystal structure types found with the different alloying partners is presented in Table 1. FeB and CrB types found with gallides, silicides and germanides have elongated trigonal prisms and the corresponding types are denoted as FeB I and CrB I. The FeB and CrB types found with rare-earth–transition-metal or Cu and Au alloys have compressed trigonal prisms and the corresponding types are denoted FeB II and CrB II. In between the two groups with different prism types are found the alloys having the CsCl structure type (for example, *R*Mg, *R*Zn) (Parthé, 1970).

Table 1. *Survey of the crystal structure types of equiatomic rare-earth–transition-metal or B metal compounds*

The arrows indicate a structure change in the series from La*M* to Lu*M*; the arrow precedes the name of the structure type found in compounds with small rare-earth elements. CrB I and FeB I compounds have elongated trigonal prisms while in CrB II and FeB II compounds they are shortened.

					*R*Si FeB I → CrB I
	*R*Ni CrB II · FeB II	*R*Cu FeB II · CsCl	*R*Zn CsCl	*R*Ga CrB I	*R*Ge FeB I → CrB I
*R*Rh CrB II · CsCl	*R*Pd CrB II · CsCl	*R*Ag CsCl	*R*Cd CsCl	*R*In CsCl	
*R*Ir CsCl	*R*Pt CrB II · FeB II	*R*Au CrB II, FeB II · CsCl	*R*Hg CsCl	*R*Tl CsCl	

The FeB and CrB structure types are geometrically closely related. It has been shown that one could obtain the FeB type from the CrB type and *vice versa* by slicing one structure into identical structural slabs and displacing these slabs sideways in a particular manner (Parthé, 1967; Hohnke & Parthé, 1966). This stacking mechanism allowed one to relate the lattice constants of the FeB type to those of the CrB type and *vice versa*. More recently, Parthé (1976) showed that both the FeB and the CrB types could be interpreted as periodically microtwinned structures according to the definitions of Andersson & Hyde (1974). The base structure for the FeB type is thereby hexagonal close-packed, whereas that for the CrB type is cubic close-packed.

The equiatomic rare-earth–nickel compounds adopt from LaNi to GdNi the CrB structure type and from DyNi to LuNi the FeB structure type (Dwight, Conner & Downey, 1965). According to Smith & Hansen (1965) YNi has a structure which is virtually identical to the FeB type. The Ni compound with Tb – in the Periodic Table between Gd and Dy – crystallizes,

0567-7408/80/040774-09$01.00

according to Lemaire & Paccard (1970), in two structure types which can be considered stacking variations of FeB and CrB, that is they can be obtained from both FeB or CrB by a particular displacement of identical structural slabs. Both TbNi types can also be interpreted by the microtwinning mechanism. The base structure for the monoclinic low-temperature modification has the stacking h_4c_2 in the Jagodzinski (1954) notation and for the orthorhombic high-temperature modification $(hc_2)_2$. The stacking of the base structures is thus intermediate between those of FeB with base-structure stacking h and CrB with stacking c (Parthé, 1976).

Another possible influence on the stacking sequence of these structural slabs was demonstrated by Gignoux & Gomez-Sal (1976) who studied the structures of pseudo-binary compounds along the line GdNi and GdCu, the first having CrB and the last CsCl types. $GdNi_{0.9}Cu_{0.1}$ has the monoclinic TbNi, low-temperature type, but $GdNi_{0.8}Cu_{0.2}$ the FeB type. Thus a gradual displacement of Ni by Cu leads to an increase in the percentage of hexagonal stacking of the close-packed base structure.

This work reports on the influence of changes in the composition of the rare-earth components on the stacking sequence in the quasi-binary sections between GdNi – the last compound crystallizing with the CrB structure type – and the Ni compounds of the smaller rare-earth elements, having the FeB structure type.

Experimental

Several samples in the sections $Gd_{1-x}Dy_xNi$ and $Gd_{1-x}Y_xNi$ (with x increasing in intervals of 0·05) were prepared from metals of high purity (Gd, Dy 99·9%; Y, Ni 99·99%). As a first step to their syntheses the binary equiatomic compounds were obtained by conventional arc-melting techniques. After their homogeneity had been confirmed by inspecting their powder diagrams they were used as master alloys for the subsequent samples. Appropriate amounts of the crushed alloys were well mixed, cold pressed and finally melted in the arc furnace under an atmosphere of purified argon. The weight of the pellets obtained (ranging from 0·5 to 1·0 g) was controlled to ensure the desired composition. The total loss was found to be less than 1%, which was considered satisfactory. The pellets were then wrapped in tantalum foil and sealed in evacuated silica capsules. Subsequent heat treatment consisted of annealing at 1073 K over a period of five weeks followed by slow cooling in the furnace.

The samples were crushed and powder diagrams of each were taken with a Guinier–de Wolff camera (Cu $K\alpha$ radiation). The inspection of the powder photographs in the quasi-binary sections clearly showed the appearance of new patterns for the compositions $Gd_{0.55}Dy_{0.45}Ni$, $Gd_{0.75}Y_{0.25}Ni$ and $Gd_{0.7}Y_{0.3}Ni$. Small single crystals, suitable for X-ray examination, could be isolated from these samples. All three crystals were found to have monoclinic unit cells with both b and c similar to those of the FeB-type compounds but with different a axes and monoclinic angles. The only systematic extinctions were those for $0k0$: $k \neq 2n$, indicating $P2_1$ and $P2_1/m$ as possible space groups. Precise lattice constants were obtained with a computer-controlled four-circle diffractometer (Philips PW 1100). The translation periods of a number of prominent reciprocal-lattice rows were measured, from which the lattice constants were determined and refined by *PARAM* (XRAY system, 1976).

Integrated intensities were collected on the same diffractometer with Ag $K\alpha$ radiation ($\lambda = 0{\cdot}5608$ Å) for $Gd_{0.75}Y_{0.25}Ni$ and for $Gd_{0.55}Dy_{0.45}Ni$ and Mo $K\alpha$ radiation ($\lambda = 0{\cdot}7107$ Å) for $Gd_{0.7}Y_{0.3}Ni$ (graphite monochromator, θ–2θ scan mode). Reflections were measured in one quadrant of reciprocal space up to $\sin\theta/\lambda$ limits of 0·70 Å^{-1} (Ag $K\alpha$) and 0·66 Å^{-1} (Mo $K\alpha$) respectively. Background corrections were applied and allowance was made for absorption by approximating the shapes of the crystals to spheres (μR being 1·2, 0·8 and 2·4 respectively).

After Lorentz and polarization corrections, equivalent reflections were averaged and unique sets of reflections were obtained. They consisted of 1307 (577 with $F_o \geq 3\sigma_F$) for $Gd_{0.75}Y_{0.25}Ni$, 1030 (552) for $Gd_{0.55}Dy_{0.45}Ni$ and 677 (490) for $Gd_{0.7}Y_{0.3}Ni$.

Determination and refinement of the crystal structures

The symmetry and cell dimensions of the three compounds supported the assumption that their crystal structures might be stacking variants of the CrB–FeB structure types. Positional parameters – using the values reported for the FeB-type LuNi (Dwight, Conner & Downey, 1965) – were calculated for some model structures (see below). After the fundamental agreement of the proposed structures had been confirmed by comparison of the Guinier photographs with calculated powder diagrams based on these models (*LAZY PULVERIX*, Yvon, Jeitschko & Parthé, 1977), the calculated positional parameters were used as starting values in a full-matrix least-squares refinement (*CRYLSQ*, XRAY system, 1976) of the single-crystal data with weights $= 1/\sigma^2(F_o)$. Scattering factors for neutral atoms (Cromer & Mann, 1968) were used and anomalous-dispersion corrections (*International Tables for X-ray Crystallography*, 1974) applied. In the refinement the positional and temperature parameters were restricted to the same values for both the rare-earth atoms. Refinement with isotropic temperature factors converged to $R = 0{\cdot}051$ for $Gd_{0.75}Y_{0.25}Ni$,

Table 2. *Crystallographic and structure data of* CrB–FeB *stacking variants*

All compounds crystallize with space group $P2_1/m$. All atoms are on equipoint 2(*e*). The rare-earth atoms are distributed statistically, the occupation ratio of the rare-earth atoms in the individual sites being identical with the ratio given by the overall chemical formula. Positional parameters are $\times 10^4$. The isotropic temperature factor is expressed as $T = \exp(-2\pi^2 U s^2)$, where $s = 1/d_{hkl}$; U values are $\times 10^4$. The values for the isotropic temperature factors are obtained by recalculation from the anisotropic ones. E.s.d.'s are in parentheses and refer to the last significant figure.

$Gd_{0.75}Y_{0.25}Ni$
h_2c_3

$a = 18{\cdot}20$ (1), $b = 4{\cdot}212$ (2), $c = 5{\cdot}506$ (1) Å, $\beta = 102{\cdot}37$ (5)°, $M_r = 198{\cdot}9$, $Z = 10$, $F(000) = 857{\cdot}5$, $D_x = 8{\cdot}01$ Mg m^{-3}, μ(Ag $K\alpha$) = 26·3 mm^{-1}, $R = 0{\cdot}043$

	x	z	U (Å^2)
R(1)	718 (1)	9186 (3)	107 (5)
R(2)	2722 (1)	8264 (3)	101 (5)
R(3)	4720 (1)	7324 (4)	111 (4)
R(4)	6718 (1)	6386 (3)	99 (5)
R(5)	8719 (1)	5426 (3)	113 (5)
Ni(1)	147 (3)	3847 (8)	130 (10)
Ni(2)	2148 (3)	2793 (9)	140 (10)
Ni(3)	4143 (3)	1833 (8)	140 (10)
Ni(4)	6142 (3)	905 (8)	130 (10)
Ni(5)	8145 (2)	9951 (8)	120 (10)

$Gd_{0.55}Dy_{0.45}Ni$
h_2c_2

$a = 14{\cdot}35$ (2), $b = 4{\cdot}217$ (1), $c = 5{\cdot}468$ (1) Å, $\beta = 100{\cdot}39$ (4)°, $M_r = 218{\cdot}3$, $Z = 8$, $F(000) = 743{\cdot}2$, $D_x = 8{\cdot}98$ Mg m^{-3}, μ(Ag $K\alpha$) = 28·4 mm^{-1}, $R = 0{\cdot}033$

	x	z	U (Å^2)
R(1)	900 (1)	9091 (2)	110 (3)
R(2)	3399 (1)	7946 (2)	108 (3)
R(3)	5902 (1)	6773 (2)	107 (3)
R(4)	8400 (1)	5582 (2)	111 (3)
Ni(1)	182 (3)	3799 (7)	128 (9)
Ni(2)	2683 (3)	2546 (7)	150 (10)
Ni(3)	5182 (3)	1359 (7)	137 (9)
Ni(4)	7681 (3)	167 (7)	130 (9)

$Gd_{0.70}Y_{0.30}Ni$
h_2c

$a = 10{\cdot}76$ (1), $b = 4{\cdot}194$ (1), $c = 5{\cdot}508$ (1) Å, $\beta = 96{\cdot}98$ (4)° $M_r = 195{\cdot}5$, $Z = 6$, $F(000) = 507$, $D_x = 7{\cdot}89$ Mg m^{-3}, μ(Mo $K\alpha$) = 50·5 mm^{-1}, $R = 0{\cdot}089$

	x	z	U (Å^2)
R(1)	1197 (3)	8955 (6)	140 (10)
R(2)	4536 (3)	7418 (6)	140 (9)
R(3)	7868 (3)	5830 (6)	150 (10)
Ni(1)	234 (8)	3810 (10)	180 (20)
Ni(2)	3575 (8)	2100 (20)	180 (20)
Ni(3)	6911 (8)	510 (20)	180 (20)

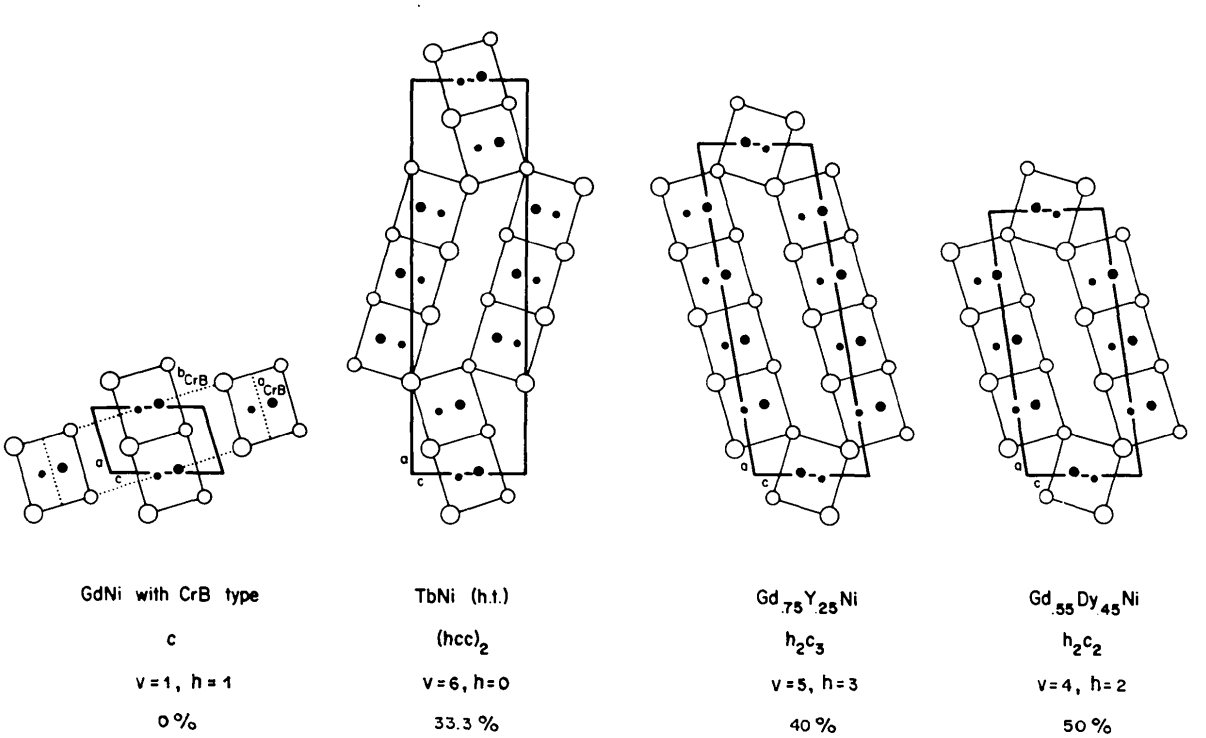

Fig. 1. The observed CrB–FeB stacking variants. Open circles correspond to rare-earth-atom sites, full circles represent the sites of the used in the text. The drawings display idealized point positions derived from periodic unit-cell twinning. The drawings are arranged

0·050 for $Gd_{0.55}Dy_{0.45}Ni$ and 0·105 for $Gd_{0.7}Y_{0.3}Ni$. At this stage anisotropic temperature factors were introduced and a correction for isotropic secondary extinction was applied giving final R values of 0·043 for $Gd_{0.75}Y_{0.25}Ni$ (932 reflections, including 355 calculating greater than the less-than threshold, $R_w = 0·047$), 0·033 for $Gd_{0.55}Dy_{0.45}Ni$ [784 (232) reflections, $R_w = 0·039$] and 0·089 for $Gd_{0.7}Y_{0.3}Ni$ [579 (89) reflections, $R_w = 0·119$].* The final structural data are presented in Table 2.

For the Y compounds, the difference of the scattering factors of Gd and Y made it promising to refine the population ratio of the rare-earth atoms on the individual sites, with the restriction that the total occupancy of each site should be unity. In the first refinement on $Gd_{0.75}Y_{0.25}Ni$ the value of the overall population ratio was fixed to agree with the assumed composition of the alloy while in the second refinement this restriction was lifted. In both cases R was unaffected, the difference of the population parameters of the individual sites being clearly smaller than the e.s.d.'s. In the second refinement the overall population ratio was insignificantly changed by <1%. These results, indicating Gd and Y disorder, were further corroborated by a model calculation, in which the Y atoms were forced to occupy preferably the hexagonal sites leading to an increase of R to 0·08.

These calculations indicate that Gd and Y atoms are randomly distributed over the different R sites and show no preference for occupying cubic or hexagonal sites as they do in their binary Ni compounds.

A drawing of the three new CrB–FeB stacking variations and the FeB, CrB and TbNi types together with the notation for the base structures according to the periodic microtwinning mechanism (Parthé, 1976) are given in Fig. 1.

* Lists of structure factors and anisotropic thermal parameters for the three compounds have been deposited with the British Library Lending Division as Supplementary Publication No. SUP 35027 (24 pp.). Copies may be obtained through The Executive Secretary, International Union of Crystallography, 5 Abbey Square, Chester CH1 2HU, England.

Geometrical conditions required by the stacking mechanism

The conditions to be derived below are, in general, not fulfilled for the majority of the FeB- and CrB-type compounds and then only one of the two types is actually found. However, in those cases where both types occur for one compound (dimorphism) or where stacking variations in quasi-binary systems are found the particular geometrical conditions are satisfied. These conditions will make it possible to relate the unit cells of the different stacking variants.

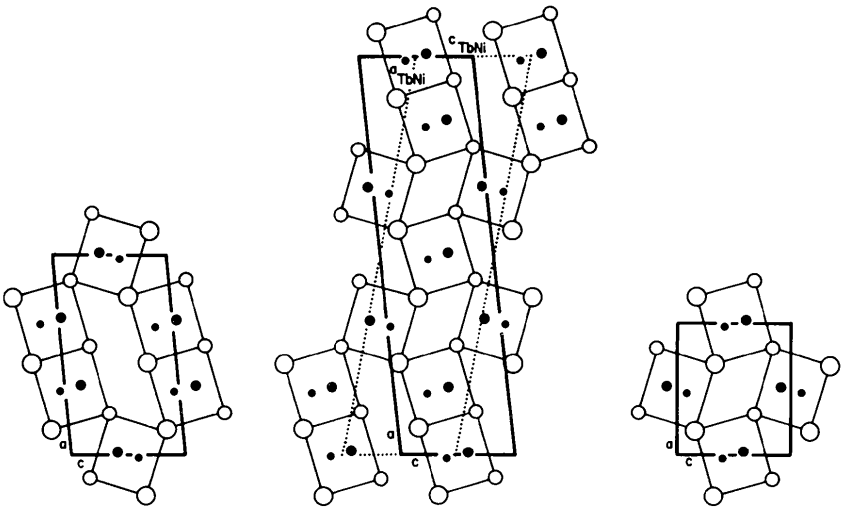

$Gd_{.7}Y_{.3}Ni$	$Gd_{.5}Dy_{.5}Ni$ with TbNi (l.t.) type	DyNi and YNi with FeB type
h_2c	h_4c_2	$(h)_2$
v = 3, h = 1	v = 6, h = 2	v = 2, h = 0
66.7%	66.7%	100%

transition-metal atoms. Small circles are at height $\frac{1}{4}$, large circles at height $\frac{3}{4}$. Dotted lines indicate cell axes which differ from the convention according to increasing percentage of hexagonal base-structure stacking; the value is indicated below each drawing.

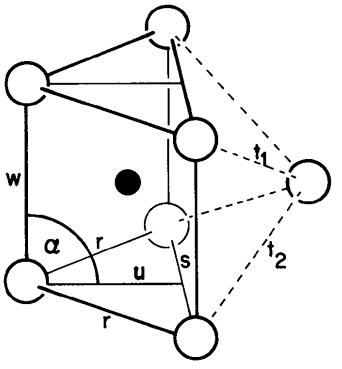

Fig. 2. The monocapped trigonal prism in the FeB–CrB structure variants.

An FeB-type structure can be considered a stacking variant of a CrB-type structure and *vice versa* if (*a*) the structural units are identical, and (*b*) the nearest-neighbour distances are identical.

The structural unit common to both types is the trigonal prism which is formed by the larger atoms (Fe, Cr) and centred by the smaller B atoms (Fig. 2). The prism base is an isosceles triangle; its legs may be denoted by r, its unique side by s, the latter corresponding to b_{FeB} and c_{CrB}. The prism height will be called w and the triangle height u, and the angle between w and u is α. The shortest prism dimensions are the triangle legs r for all kinds of CrB- and FeB-type compounds.

A trigonal prism is characterized by three quantities: the ratios w/s, w/u and α.

The ratio w/s may vary widely among different compounds. It was used – actually in the form of the ratios a_{FeB}/b_{FeB} or a_{CrB}/c_{CrB}, which depend on it – to distinguish between group I and group II compounds (Table 1). The ratio w/s and, further, $b_{FeB} = c_{CrB}$ have to be the same for stacking variants.

When $\alpha = 90°$ the prism is orthogonal. In the CrB structure the prisms are necessarily orthogonal for symmetry reasons. The requirement, according to condition (*a*), of orthogonal prisms in the FeB-type structure also leads to the relation

$$\frac{a_{FeB}^2}{c_{FeB}^2} = \frac{1 - 4z_{Fe}}{1 - 4x_{Fe}}. \tag{1}$$

A study of the FeB- and CrB-type structures reveals that each B atom is at the centre of a monocapped prism, the atom at the cap's apex belonging to a neighbouring trigonal prism. Symmetry determines that in the CrB-type structure the distances from prism corners to the capping atom, t_1 and t_2, are equal. In view of condition (*b*) the same is required for the FeB-type structure. Equality, $t_1 = t_2$, is met when

$$\frac{a_{FeB}^2}{c_{FeB}^2} = \frac{16z_{Fe}^2 - 1}{1 - 8x_{Fe}}. \tag{2}$$

The combining of (1) and (2) yields

$$z_{Fe} = \frac{6x_{Fe} - 1}{2(1 - 4x_{Fe})}. \tag{3}$$

If this condition is met in an FeB phase, then the distances $t_1 = t_2$ and r must necessarily be equal. As a consequence of this, each prism-forming atom now has six nearest neighbours of the same kind at the same distance. Since this in turn must also be valid for a corresponding CrB-type structure, the y_{Cr} parameter of the latter can be expressed in terms of the axial ratio

$$y_{Cr} = \tfrac{1}{8}(1 + a_{CrB}^2/b_{CrB}^2). \tag{4}$$

For FeB- and CrB-type structures to be stacking variants, w/s and w/u must, therefore, be the same and α must be 90°. This allows one to set up relations for the axial ratios. The stacking is conveniently presented in a plane normal to s, *i.e.* normal to b_{FeB} or c_{CrB} respectively. Let us draw in this plane the two mutually perpendicular prism vectors $\mathbf{w}$ and $\mathbf{u}$ with absolute values $|\mathbf{w}| = w$ and $|\mathbf{u}| = u$ (Fig. 3). It can be seen that the axial ratios a_{FeB}/c_{FeB} and a_{CrB}/b_{CrB} can be related to the prism ratio w/u according to

$$\frac{a_{FeB}}{c_{FeB}} = \frac{2|\mathbf{w}|\cos\psi}{2|\mathbf{u}|\cos\psi} = \frac{w}{u}, \tag{5}$$

$$\frac{a_{CrB}}{b_{CrB}} = \frac{|\mathbf{w}|}{2\left\{|\mathbf{u}| + \left[|\mathbf{u}|^2 - \left(\frac{|\mathbf{w}|}{2}\right)^2\right]^{1/2}\right\}} = \frac{\frac{w}{u}}{2\left\{1 + \left[1 - \left(\frac{1}{2}\frac{w}{u}\right)^2\right]^{1/2}\right\}} = \frac{1 - \left[1 - \left(\frac{1}{2}\frac{w}{u}\right)^2\right]^{1/2}}{\frac{1}{2}\frac{w}{u}}. \tag{6}$$

(Note that since $r = t_1 = t_2$, their projections on the plane are also equal, *i.e.* $|\mathbf{u}|$.)

However, these equations are not easy to apply and it appears more convenient to express the relations, rather, in terms of the angle ψ instead of w/u. According to Fig. 3

$$\frac{w}{u} = 2\sin 2\psi. \tag{7}$$

Equations (5) and (6) can now be expressed in terms of ψ. These equations are later used to calculate, in turn, the angle ψ.

$$\frac{a_{FeB}}{c_{FeB}} = 2\sin 2\psi \tag{8}$$

$$\frac{a_{CrB}}{b_{CrB}} = \text{tg } \psi. \tag{9}$$

For a stacking pair equality of w/u, and with it equality of ψ, is required. With the help of Fig. 3 it is now possible to derive the following simple unit-cell relations

$$a_{CrB} = \frac{a_{FeB}}{2 \cos \psi} \tag{10}$$

$$b_{CrB} = \frac{a_{FeB}}{2 \sin \psi}, \tag{11}$$

to which we add the relation already discussed above

$$c_{CrB} = b_{FeB}. \tag{12}$$

The previously published unit-cell relations for FeB and CrB stacking pairs were different in as far as they did not relate to the angle ψ or the prism ratio w/u and thus cannot be extended to apply to the more complicated stacking variations.

The applicability of these equations has been tested for those compounds where both structure types have been found experimentally, *e.g.* DySi, HoSi, ErSi, PrGe ($\psi \sim 22°$) (Hohnke & Parthé, 1966), LaAu, CeAu, PrAu, NdAu, SmAu (McMasters, Gschneidner, Bruzzone & Palenzona, 1971) and PrPt, NdPt ($\psi \sim 19{\cdot}5°$) (LeRoy, Moreau, Paccard & Parthé, 1978).

The adjustable parameters of the metal atoms can also be expressed in terms of ψ. The additional assumption that the B atoms centre the trigonal prisms – six equal distances to the surrounding atoms forming the trigonal prism – allows one to calculate the B atom point positions as well.

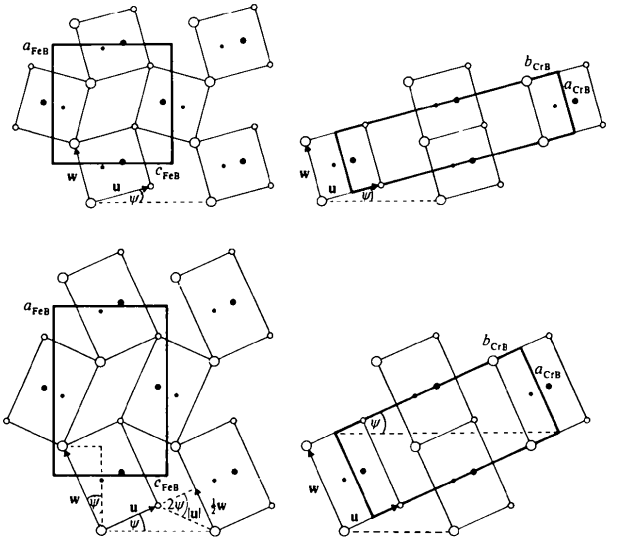

Fig. 3. Two FeB–CrB structure pairs for different values of w/u and ψ respectively. Upper pair: $w/u = 1$ and $\psi = 15°$; lower pair: $w/u = 1{\cdot}5$ and $\psi = 24{\cdot}3°$.

FeB *with Pnma*: Fe *and* B *in* 4(*c*)

$$x_{Fe} = \frac{1}{4} - \frac{1}{16 \cos^2 \psi} \tag{13a}$$

$$x_B = \frac{1}{16} \frac{b_{FeB}^2}{c_{FeB}^2} \tag{13b}$$

$$z_{Fe} = \tfrac{1}{4} - \sin^2 \psi \tag{14a}$$

$$z_B = \tfrac{1}{2} + 4 \cos^2 \psi \times x_B. \tag{14b}$$

CrB *with Cmcm*: Cr *and* B *in* 4(*c*)

$$y_{Cr} = \frac{1}{8 \cos^2 \psi} \tag{15a}$$

$$y_B = \tfrac{1}{2} - \tfrac{1}{2} \sin^2 \psi \times \frac{c_{CrB}^2}{a_{CrB}^2}. \tag{15b}$$

Table 3. *Interatomic distances* (Å) *in* $Gd_{0.75}Y_{0.25}Ni$ *with base-structure stacking* h_2c_3 *up to* 4 Å

E.s.d.'s are in parentheses: $R \equiv Gd_{0.75}Y_{0.25}$; redundant distances are omitted.

Ni(1)–2 Ni(1)	2·574 (4)	Ni(5)– *R*(4)	2·899 (5)
Ni(1)– Ni(2)	3·809 (7)	Ni(5)– *R*(5)	2·901 (5)
Ni(1)– Ni(5)	3·813 (6)	Ni(5)–2 *R*(1)	2·920 (4)
Ni(1)– *R*(1)	2·900 (5)	Ni(5)–2 *R*(2)	2·925 (4)
Ni(1)– *R*(5)	2·912 (6)	Ni(5)– *R*(5)	2·972 (5)
Ni(1)–2 *R*(5)	2·915 (4)		
Ni(1)–2 *R*(1)	2·929 (3)	*R*(1)–2 *R*(5)	3·603 (2)
Ni(1)– *R*(1)	2·968 (8)	*R*(1)–2 *R*(5)	3·612 (3)
		R(1)–2 *R*(1)	3·616 (3)
Ni(2)–2 Ni(5)	2·580 (4)	*R*(1)– *R*(5)	3·781 (3)
Ni(2)– Ni(3)	3·779 (7)	*R*(1)– *R*(2)	3·789 (4)
Ni(2)– *R*(2)	2·903 (6)		
Ni(2)–2 *R*(4)	2·914 (4)	*R*(2)–2 *R*(4)	3·587 (2)
Ni(2)– *R*(1)	2·917 (5)	*R*(2)–2 *R*(4)	3·625 (2)
Ni(2)–2 *R*(5)	2·924 (4)	*R*(2)–2 *R*(5)	3·628 (3)
Ni(2)– *R*(2)	2·969 (5)	*R*(2)– *R*(3)	3·780 (4)
Ni(3)–2 Ni(4)	2·577 (4)	*R*(3)–2 *R*(3)	3·588 (2)
Ni(3)– Ni(4)	3·780 (7)	*R*(3)–2 *R*(3)	3·625 (3)
Ni(3)– *R*(2)	2·893 (5)	*R*(3)–2 *R*(4)	3·629 (3)
Ni(3)– *R*(3)	2·896 (6)	*R*(3)– *R*(4)	3·781 (4)
Ni(3)–2 *R*(4)	2·918 (4)		
Ni(3)–2 *R*(3)	2·919 (4)	*R*(4)– *R*(5)	3·790 (4)
Ni(3)– *R*(3)	2·980 (5)		
Ni(4)– Ni(5)	3·793 (7)		
Ni(4)– *R*(3)	2·898 (5)		
Ni(4)– *R*(4)	2·900 (6)		
Ni(4)–2 *R*(3)	2·916 (4)		
Ni(4)–2 *R*(2)	2·918 (4)		
Ni(4)– *R*(4)	2·975 (5)		

Unit-cell relationship for the CrB–FeB stacking variants

In order to derive unit-cell relationships for the new stacking variations one has to verify first that the geometrical conditions for stacking are satisfied. Since all the rare-earth elements in the ternary alloys have about the same size and since all the monoclinic unit cells have similar b and c values, it is safe to assume that the trigonal prisms have similar dimensions and the structures similar ψ angles. In the ideal case each prism-forming atom should have six equidistant neighbours of the same kind. Examination of the interatomic distances in Tables 3, 4 and 5 shows that six shortest R–R and six shortest Ni–R distances vary in each group by $<1{\cdot}5\%$.

A study of the CrB–FeB stacking variations in Fig. 1 shows that the a and β values of the unit cells depend on the particular stacking of the trigonal prisms while the b and c values are essentially the same as for the FeB type. The a value obviously corresponds to the value of a resultant vector formed by summing the prism-edge vectors **w** of the different prisms stacked along **a**. Each individual prism-edge vector **w** has a vertical component with absolute value $a_{FeB}/2$ and a positive or negative horizontal component with absolute value $(a_{FeB}/2)\,\mathrm{tg}\,\psi$. If the structure is characterized by v linked prisms along **a** the resultant vector will have a vertical component with absolute value $v(a_{FeB}/2)$ and a horizontal component with absolute value $h(a_{FeB}/2)\,\mathrm{tg}\,\psi$. h is the number of resultant horizontal prism components. It is smaller than v if there are horizontal prism vector components which cancel each other in pairs. For example, for FeB: $v = 2$, $h = 0$.

Hence,

$$a = \frac{a_{FeB}}{2}(v^2 + h^2\,\mathrm{tg}^2\,\psi)^{1/2}, \qquad (16a)$$

$$b = b_{FeB}, \qquad (16b)$$

$$c = c_{FeB}, \qquad (16c)$$

$$\mathrm{tg}\,(\beta - 90) = \frac{h}{v}\,\mathrm{tg}\,\psi. \qquad (16d)$$

If h is zero, then $\beta = 90°$ and the corresponding structure is orthorhombic or pseudo-orthorhombic. If $h \neq v$, then, because the horizontal components cancel in pairs, $v - h$ must be even and hence h and v will always have the same parity.

Table 4. *Interatomic distances* (Å) *in* $Gd_{0.55}Dy_{0.45}Ni$ *with base-structure stacking* h_2c_2 *up to* 4 Å

E.s.d.'s are in parentheses; $R \equiv Gd_{0.55}Dy_{0.45}$; redundant distances are omitted.

Ni(1)–2 Ni(1)	2·587 (3)	Ni(4)– R(3)	2·873 (5)
Ni(1)– Ni(2)	3·773 (7)	Ni(4)– R(4)	2·878 (4)
Ni(1)– Ni(4)	3·776 (6)	Ni(4)–2 R(1)	2·909 (3)
Ni(1)– R(1)	2·891 (4)	Ni(4)–2 R(2)	2·913 (3)
Ni(1)– R(4)	2·898 (5)	Ni(4)– R(4)	2·955 (4)
Ni(1)–2 R(4)	2·907 (3)		
Ni(1)–2 R(1)	2·911 (3)	R(1)–2 R(4)	3·589 (2)
Ni(1)– R(1)	2·940 (4)	R(1)–2 R(4)	3·594 (2)
		R(1)–2 R(1)	3·610 (3)
Ni(2)–2 Ni(4)	2·577 (3)	R(1)– R(2)	3·750 (5)
Ni(2)– Ni(3)	3·757 (7)	R(1)– R(4)	3·751 (4)
Ni(2)– R(2)	2·883 (4)		
Ni(2)– R(1)	2·894 (5)	R(2)–2 R(3)	3·570 (2)
Ni(2)–2 R(3)	2·904 (3)	R(2)–2 R(4)	3·610 (3)
Ni(2)–2 R(4)	2·913 (3)	R(2)–2 R(3)	3·612 (2)
Ni(2)– R(2)	2·946 (4)	R(2)– R(3)	3·762 (5)
Ni(3)–2 Ni(3)	2·578 (3)	R(3)–2 R(3)	3·619 (3)
Ni(3)– Ni(4)	3·759 (7)	R(3)– R(4)	3·757 (5)
Ni(3)– R(3)	2·880 (4)		
Ni(3)– R(2)	2·883 (5)		
Ni(3)–2 R(2)	2·909 (3)		
Ni(3)–2 R(3)	2·912 (3)		
Ni(3)– R(3)	2·955 (4)		

Table 5. *Interatomic distances* (Å) *in* $Gd_{0.7}Y_{0.3}Ni$ *with base-structure stacking* h_2c *up to* 4 Å

E.s.d.'s are in parentheses; $R \equiv Gd_{0.7}Y_{0.3}$; redundant distances are omitted.

Ni(1)– R(1)	2·899 (9)	Ni(3)– R(3)	2·892 (9)
Ni(1)– R(3)	2·90 (1)	Ni(3)– R(2)	2·894 (9)
Ni(1)–2 R(3)	2·917 (7)	Ni(3)–2 R(1)	2·913 (6)
Ni(1)–2 R(1)	2·918 (6)	Ni(3)–2 R(2)	2·924 (7)
Ni(1)– R(1)	2·981 (9)	Ni(3)– R(3)	2·984 (9)
Ni(1)–2 Ni(1)	2·558 (7)		
Ni(1)– Ni(3)	3·81 (1)	R(1)–2 R(3)	3·600 (3)
Ni(1)– Ni(2)	3·82 (1)	R(1)–2 R(3)	3·601 (4)
		R(1)–2 R(1)	3·617 (5)
Ni(2)– R(2)	2·895 (9)	R(1)– R(3)	3·781 (6)
Ni(2)–2 R(2)	2·910 (6)	R(1)– R(2)	3·790 (6)
Ni(2)– R(1)	2·912 (9)		
Ni(2)–2 R(3)	2·921 (7)	R(2)–2 R(2)	3·577 (4)
Ni(2)– R(2)	2·983 (9)	R(2)–2 R(2)	3·625 (4)
Ni(2)–2 Ni(3)	2·562 (7)	R(2)–2 R(3)	3·628 (4)
Ni(2)– Ni(3)	3·80 (1)	R(2)– R(3)	3·793 (6)

Construction of a starting model

Once the symmetry and dimensions of the unit cell have been established [a, b, c, β for $P2_1/m$ or a, b, c ($\beta = 90°$) for $Pnma$] the value for v can be calculated from

$$v = \frac{2a\cos(\beta - 90)}{a_{FeB}} \qquad (17a)$$

or

$$v = \frac{a\cos(\beta - 90)}{c\sin 2\psi}. \qquad (17b)$$

The approximate a_{FeB} and ψ values are known from one of the binary end members. Due to the presence of atoms of slightly different size in the ternary alloys the corresponding a_{FeB} and ψ values may be slightly different. Since v has to be an integer, (17) allows one to obtain the precise values of a_{FeB} and ψ for the ternary alloy which will be used for the later calculations.

The value of h can be obtained with (16*d*). If, however, the h value obtained is not an integer† the chosen unit cell does not agree with the unit cell defined by (16) and has to be transformed. On the assumption that a' and β' are measured cell constants which give a non-integral h value, (18) has to be applied for different integral values of n such that h is an integer smaller than v (except $v = 1$) and of the same parity as v.

$$h = \frac{a' \sin(\beta' - 90) + nc}{\frac{a_{FeB}}{2} \operatorname{tg} \psi}, \quad n = 0, \pm 1, \pm 2, \ldots. \quad (18)$$

If the correct n value is labelled as n^* the new a and β values can be calculated according to

$$\operatorname{tg}(\beta - 90) = \frac{|a' \sin(\beta' - 90) + n^* c|}{a' \cos(\beta' - 90)} \quad (19)$$

and

$$a = \frac{a' \cos(\beta' - 90)}{\cos(\beta - 90)}. \quad (20)$$

As an example we may consider the published unit-cell data for the low-temperature modification of TbNi (Lemaire & Paccard, 1970) with a unit cell indicated by dotted lines in Fig. 1. With $v = 6$ and $\psi = 20{\cdot}07°$ obtained from (17), one calculates from (16*d*) a value of 2·14 for h. Thus the unit cell has to be transformed. With $n^* = -1$ one obtains a value for h which is close to 2. Thus for the TbNi low-temperature structure $v = 6$ and $h = 2$.

Once v and h are known the structure is fully determined provided that $v < 5$. For higher v values multiple solutions are possible.

For the calculation of the fractional coordinates of a model structure we note that the x parameters of the atoms do not depend on the stacking sequence. If a unit-cell origin similar to that used for drawing the unit cells in Fig. 1 is chosen, the jth coordinate may be defined as:

$$x^j = \frac{2}{v}\left(x_{FeB} + \frac{j-1}{2}\right), \quad \text{where } 1 \le j \le v. \quad (21)$$

Insertion of (13*a*) or (13*b*) for x_{FeB} gives the wanted x_R^j and x_T^j coordinates respectively.

† After due consideration of the possible errors which affect the measured unit-cell data.

In the calculation of the z parameters of a model structure the stacking sequence is important. It is advisable to arrange the sequence in an orthogonal pseudo-cell with $a_o = a \sin\beta$ (b and c remaining unchanged). The first value for z_R for the rare-earth atom can be obtained by (14*a*). Each stacking displacement in z for a rare-earth atom is given by $\frac{1}{2} - 2z_R$ which has to be added to or subtracted from the z value of the preceding rare-earth atom.

The z_T parameter of the first transition-metal atom is found analogously from (14*b*). However, the amount of shift in the stacking step now depends on the preceding rare-earth atom, being $\pm(\frac{1}{2} - 2z_R)$ if the latter is in a cubic position and $\pm(\frac{1}{2} - 2z_T)$ if it is in a hexagonal position. Once the atomic parameters are calculated, a retransformation into the true monoclinic cell has to be made. Before the transformation it might be necessary to change the signs of all z values in order to ensure that the corresponding monoclinic unit cell has $\beta > 90°$.

Change of stacking sequence with composition

For the derivation of the unit cells and for a general characterization of the different CrB–FeB stacking variations we have used the particular sequence of the prism-edge vectors. Since all the new structure types can be interpreted by microtwinning of close-packed base structures it is possible to characterize these structures by describing the stacking sequence of the close-packed base structures. In Fig. 1 the base-structure stacking is indicated by means of the Jagodzinski notation together with the corresponding percentage of hexagonal stacking. In the quasi-binary system GdNi–YNi the structures of GdNi, $Gd_{0.75}Y_{0.25}Ni$, $Gd_{0.7}Y_{0.3}Ni$ and YNi have the following percentages of hexagonal stacking: 0, 40, $66\frac{2}{3}$, 100%. In the quasi-binary system GdNi–DyNi with the phases GdNi, $Gd_{0.55}Dy_{0.45}Ni$, $Gd_{0.5}Dy_{0.5}Ni$, DyNi the corresponding values are 0, 50, $66\frac{2}{3}$, 100%.* One notes that the type of stacking or the ratio of FeB to CrB fragments in the structure depends on the composition. Structures of compounds with compositions closer to the binary compound with CrB type (0% hexagonal stacking) have a smaller percentage of hexagonal stacking whereas those closer to FeB type (100% hexagonal stacking) have a higher percentage.

We acknowledge the helpful comments of Dr M. G. Vincent. This study was supported by the Swiss National Science Foundation under project No. 2.250-0.79.

* Here we have included the phase $Gd_{0.5}Dy_{0.5}Ni$ with the TbNi, low-temperature structure type. Its structural details together with the homogeneity ranges of all phases mentioned above will be presented elsewhere (Klepp & Parthé, to be published).

References

ANDERSSON, S. & HYDE, B. G. (1974). *J. Solid State Chem.* **9**, 92–101.

CROMER, D. T. & MANN, J. B. (1968). *Acta Cryst.* A**24**, 321–324.

DWIGHT, A. E., CONNER, R. A. JR & DOWNEY, J. W. (1965). *Acta Cryst.* **18**, 835–839.

GIGNOUX, D. & GOMEZ-SAL, J. C. (1976). *J. Magn. Magn. Mater.* **1**, 203–213.

HOHNKE, D. & PARTHÉ, E. (1966). *Acta Cryst.* **20**, 572–582.

International Tables for X-ray Crystallography (1974). Vol. IV. Birmingham: Kynoch Press.

JAGODZINSKI, H. (1954). *Acta Cryst.* **7**, 17–25; *Neues Jahrb. Mineral. Abh.* **10**, 49–65.

LEMAIRE, R. & PACCARD, D. (1970). *J. Less-Common Met.* **21**, 403–413.

LEROY, J., MOREAU, J.-M., PACCARD, D. & PARTHÉ, E. (1978). *Acta Cryst.* B**34**, 9–13.

MCMASTERS, O. D., GSCHNEIDNER, K. A. JR, BRUZZONE, G. & PALENZONA, A. (1971). *J. Less-Common Met.* **25**, 135–160.

PARTHÉ, E. (1967). *Colloq. Int. CNRS*, **157**, 195–205.

PARTHÉ, E. (1970). *Colloq. Int. CNRS*, **180**, 61–79.

PARTHÉ, E. (1976). *Acta Cryst.* B**32**, 2813–2818.

SMITH, J. F. & HANSEN, D. A. (1965). *Acta Cryst.* **18**, 60–62.

XRAY system (1976). Tech. Rep. TR-446. Computer Science Center, Univ. of Maryland, College Park, Maryland.

YVON, K., JEITSCHKO, W. & PARTHÉ, E. (1977). *J. Appl. Cryst.* **10**, 73–74.

Acta Cryst. (1980). B**36**, 782–785

The Structures of Potassium Lead Triiodide Dihydrate and Ammonium Lead Triiodide Dihydrate

BY DORA BEDLIVY* AND K. MEREITER

Institut für Mineralogie, Kristallographie und Strukturchemie, Technische Universität Wien, A-1060 Vienna, Austria

(*Received* 25 *October* 1979; *accepted* 3 *December* 1979)

Abstract

$KPbI_3.2H_2O$, $NH_4PbI_3.2H_2O$ and $RbPbI_3.2H_2O$ are isostructural and crystallize in space group *Pnma* with $Z = 4$. $KPbI_3.2H_2O$: $a = 10{\cdot}168$ (2), $b = 4{\cdot}577$ (1), $c = 22{\cdot}484$ (5) Å. $NH_4PbI_3.2H_2O$: $a = 10{\cdot}262$ (2), $b = 4{\cdot}611$ (1), $c = 22{\cdot}613$ (5) Å. $RbPbI_3.2H_2O$: $a = 10{\cdot}276$ (5), $b = 4{\cdot}715$ (3), $c = 22{\cdot}623$ (9) Å. The structures of the first two compounds have been determined and refined to $R = 0{\cdot}030$ and $R = 0{\cdot}039$, respectively. The structures contain $[PbI_3]^-$ double chains of edge-sharing PbI_6 octahedra. The chains extend along **b** and are connected by alkali ions and water molecules. Pb–I bonds average 3·241 Å. The structures can be regarded as hydrated variants of the NH_4CdCl_3 structure type, in which anhydrous $RbPbI_3$ and $CsPbI_3$ are known to crystallize. Close relationships to the structures of $NH_4HgCl_3.H_2O$ and $NaHgCl_3.2H_2O$ are noted.

Introduction

PbI_2 is only slightly soluble in water but dissolves readily in hot concentrated aqueous solutions of alkali iodides. On evaporation or cooling of the solutions, $APbI_3.nH_2O$ double salts are obtained, where A = Li, Na, K, NH_4, Rb or Cs and n = 0, 2 or 4, depending on the alkali ion and, in part, on the conditions of formation (*Gmelins Handbuch der Anorganischen Chemie*, 1970). Of this family, only the structures of the two isotypic anhydrous salts $RbPbI_3$ (Haupt, Huber & Preut, 1974) and $CsPbI_3$ (low-temperature form; Møller, 1959) are known. In this work we present the crystal structures of $KPbI_3.2H_2O$ and $NH_4PbI_3.2H_2O$, together with crystal data for $RbPbI_3.2H_2O$.

Experimental

Crystals of the NH_4 and K salts were obtained by saturating solutions of alkali iodide (50 wt% in water) with PbI_2 at 353 K and cooling them slowly to 313 K. When we applied this method for the Rb salt we obtained only anhydrous $RbPbI_3$, a simple preparation method not, however, known in the literature. We finally obtained the desired dihydrate by crystallization at room temperature.

$KPbI_3.2H_2O$, $NH_4PbI_3.2H_2O$ and $RbPbI_3.2H_2O$ are isomorphous; they form thin flexible pale-yellow needles. The crystals are very similar in habit to anhydrous $RbPbI_3$ and $CsPbI_3$, the only obvious

* Permanent address: Departamento de Ciencias Geológicas, FCEN Universidad Buenos Aires, 1428 Buenos Aires, Argentina.

0567-7408/80/040782-04$01.00